Journal of the European Ceramic Society 19 (1999) 2747–2756

PII: S0955-2219(99)00035-7
0955-2219/99/$ - see front matter

The Effect of Thermal Cycling on Oxide Scale Structure and Morphology on a Hot-pressed Silicon Nitride

F. A. Costa Oliveira† and D. J. Baxter*

European Commission—DG Joint Research Centre, Institute for Advanced Materials, PO Box 2, NL-1755 ZG Petten, The Netherlands

(Received 12 October 1998; accepted 10 January 1999)

Abstract

Dense Si_3N_4 hot-pressed with the aid of 9 wt% Y_2O_3 was oxidised in 'dry' synthetic air at both 1000 and 1200°C for up to 500 h under thermal cycling conditions. The experiments revealed that thermal cycling has little effect on oxidation kinetics although the morphology of surface oxidation products is affected by the cycling frequency. Cracks formed in the oxide layers on cooling healed immediately on re-exposure to high temperature, and there was no apparent change in the oxidation rate controlling mechanism over the time period investigated. The exposure of the material at 1000°C did not result in catastrophic oxidation as observed for some other Y_2O_3-doped hot-pressed Si_3N_4 compositions. Additionally, it was observed that crystallisation of the oxide layer with time (assisted in part by the outward diffusion of intergranular phase cations from the bulk ceramic to the surface scale) leads to non-parabolic kinetics owing to reduced rates of diffusion through crystalline phases in the surface scale. © *1999 Elsevier Science Ltd. All rights reserved*

Keywords: impurities, corrosion, Si_3N_4, thermal cycling.

1 Introduction

Many potential applications of silicon nitride ceramics involve high temperature exposure to oxidising environments. These materials are inherently unstable with respect to oxidation and form a thin protective layer of silicon dioxide that acts as a reaction barrier owing to the low oxygen mobility in SiO_2.[1]

In a power generator turbine or heat exchanger type of application, a structural component may be subjected to essentially isothermal conditions for prolonged periods of time. Other applications, including aircraft turbines or internal combustion engines, involve frequent thermal cycling and very large temperature gradients. In all these applications, oxidation resistance is of major concern.

In the continuing search for materials possessing excellent high temperature properties, namely high strength and corrosion resistance, considerable effort has been devoted towards the development of low density advanced ceramics (including both monolithic and composite ceramics, e.g. silicon nitride-based ceramics). Compared to their metallic counterparts commonly in use in heat engines, these materials allow higher operating temperatures, thus facilitating completely uncooled use under very aggressive environmental conditions, with the possibility of increased rotational speeds, giving higher pressure ratios, and thus potentially higher efficiencies can be achieved.

Most research work on the oxidation behaviour of silicon-based ceramics has been concerned with isothermal exposures for short times, typically of the order of several hours. There have been few studies devoted to the effect of thermal cycling on oxidation of silicon-based ceramics, despite the fact that SiO_2, the main oxidation product, undergoes a number of phase transformations on heating and cooling. Therefore, mismatch between the thermal expansion coefficients of the bulk ceramic and the oxide layer may lead to tensile stresses and eventually cracking of the otherwise protective oxide scale. The purpose of the present work was to assess the effect of such cracking on the oxidation kinetics.

*To whom correspondence should be addressed. Fax: +31-224-563841; e-mail: baxter@jrc.nl
†On leave from INETI, Instituto Nacional de Engenharia e Tecnologia Industrial, Estrada do Paço do Lumiar, 1699 Lisboa Codex, Portugal.

Weaver and Lucek[2] have investigated the effect of cyclic oxidation on the weight change data of a hot-pressed Si_3N_4 doped with 8 wt% Y_2O_3, at temperatures ranging from 1000 to 1300°C for a total exposure time of 96 h. Weight gains for specimens removed from the furnace every 24 h were comparable to those obtained for isothermal oxidation. However, nothing is said about the effect of thermal cycling on the morphology of the oxide layer.

Maeda *et al.*[3] have studied a hot-pressed Si_3N_4 doped with Y_2O_3 and Al_2O_3 at 1200°C for up to 3000 h. Weight gains were comparable to those obtained for 1470 h and 3000 h of isothermal exposure. No noticeable difference in morphology of the oxide scales was observed between samples cycled and isothermally exposed. However, they have noticed a change in the parabolic rate after 270 h of exposure. They attribute this to various microstructural changes which occur in the scale with time, e.g. crystallisation of amorphous phases within the scale and viscosity changes of the oxidation products owing to migration of both additives and impurities from the bulk to the oxide scale.

Echeberria and Castro[4] have examined the cyclic oxidation behaviour of a dense silicon nitride doped with 1 wt% Y_2O_3 and did not observe any substantial difference in oxidation kinetics between isothermal and cyclic exposures in air in the temperature range of 1400 to 1500°C up to 72 h. The major difference was observed in the morphology of the oxide layers, particularly in the size of the β-$Y_2Si_2O_7$ crystals (being larger in the case of cyclic oxidation). The reasons for this are not clear.

Despite the limited number of studies on cyclic oxidation of silicon-based ceramics, data available indicate that Si_3N_4 performs relatively well under thermal cycling conditions. However, there are still some questions, which remain unanswered.

Although the use of Y_2O_3 produces significantly improved mechanical properties at high temperatures (> 1300°C) compared with MgO-doped hot-pressed materials,[2,5] some compositions of Si_3N_4 hot-pressed with Y_2O_3 are prone to fail catastrophically at temperatures in the range 90–1200°C in oxidising environments.[6,7] This is attributed to oxidation of some unstable quaternary crystalline intergranular phases formed on sintering, resulting in substantial increases in molar volume,[8] which may, eventually, lead to extensive cracking. At higher temperatures (> 1200°C), however, this problem is not observed, due to the more protective character of the oxide layer formed which is derived from the softening of both the oxide layer and the intergranular phase allowing easier deformation for the relief of oxidation-induced stresses. On this basis, it is therefore convenient to evaluate the oxidation behaviour of Y_2O_3-doped hot-pressed Si_3N_4 at lower temperatures (e.g. 1000°C) under cyclic conditions to assess whether cracking of the oxide layer influences the oxidation rate or not.

The aim of the work was to evaluate the influence of thermal cycling on both the oxidation kinetics and the morphology of the oxide layers. This paper highlights the results of an investigation of the oxidation behaviour of a yttria-doped silicon nitride under cycling thermal conditions and illustrates the importance of relying on microstructural evaluation in order to assess the reliability of mathematical models fitted to oxidation rates.

2 Experimental

2.1 Material

The material under investigation was a commercial silicon nitride grade designated Ceranox NH209 (ex. Feldmühle AG, now Ceramtec, Germany). According to the manufacturer, this material has been hot-pressed at 1750°C under a pressure of 40 MPa using 9·0 wt% Y_2O_3 and 1·7 wt% Fe_2O_3 to a bulk density of 3·33 Mg m^{-3} and 2% open porosity.

The microstructure of Ceranox NH209 consists primarily of prismatic hexagonal grains of β-Si_3N_4 surrounded by a crystalline phase identified as $Y_{10}(SiO_4)_6N_2$ (also known as H-phase). By means of electron microdiffraction analysis in a TEM, some pockets of $YNSiO_2$ (known as K-phase) as well as $FeSi_2$ inclusions were also found. Detailed characterisation of this material is described elsewhere.[9] Test bars were diamond cut to 3×4×15 mm (edges chamfered to 0·12×45°) and ground on all faces to a surface roughness of 0·2 μm (R_a).

2.2 Oxidation testing and evaluation

Prior to testing, the dimensions of the samples were measured (accuracy of ± 0·002 mm). The samples were ultrasonically cleaned in ethanol for 30 min, dried in a desiccator for at least 10 h and finally weighed (accuracy of ± 10 μg).

Oxidation tests were carried out using a purpose-built, controlled atmosphere, programmable thermal cycling facility. The facility consists of hot and cold zones and the automated movement of specimens between the two enables heating at approximately 200°C min^{-1} and cooling to approximately 100°C within 10 min. The specimens were supported using Pt wire on a high purity recrystallised alumina (> 99·9%) carrier. All other furnace internals in the hot zone were also made from high purity alumina. Tests were carried out in flowing 'dry' synthetic air (< 5 ppm H_2O) at a rate of 3 l h^{-1} and a pressure of 0·12 MPa.

Weight change data versus time was recorded for three sets of experiments:

(a) Oxidation times of 25 h at 1000 or 1200°C for a total of 150 h (six cycles) with cooling to room temperature after each cycle for the purpose of specimen weighing.
(b) Oxidation at 1000 or 1200°C for 6·25 h each cycle with specimen weighing after every four cycles (i.e. every 25 h accumulated time) to a total exposure time of 150 h. One additional test was extended to 500 h of exposure at 1000°C.
(c) Oxidation at 1200°C for 1 h each cycle with specimen weighing after every 25 cycles (i.e. every 25 h accumulated time) to a total exposure time of 150 h.

Specimens were cooled to room temperature for the purpose of weighing. During continuous cycling to accumulate 25 h between interruptions for weighing, specimens were cooled to approximately 100°C in the sealed furnace.

Bulk identification of the oxidation products was carried out by XRD and scanning electron microscopy (SEM) together with an EDX analyser.

3 Results and Discussion

3.1 Oxidation behaviour

The data in Fig. 1 show that there is no significant difference between weight changes for specimens cycled six times or 24 times during the 150 h at each test temperature. Additionally, samples cycled 150 times (1 h holding time cycles) at 1200°C showed similar weight changes to those observed for specimens cycled six times or 24 times. Microstructural examination showed that cracking of the surface scale occurred on all test pieces regardless of experimental parameters. It can be inferred that these cracks, formed during cooling from the high temperature, either did not penetrate to the ceramic surface, or that healing occurred quickly upon re-exposure at high temperature preventing a sustained acceleration in the rate of oxidation. Therefore, the effect of thermal cycling on the kinetics of oxidation at both 1000 and 1200°C is negligible within the range of conditions used in this work. In addition, this material does not exhibit rapid oxidation of the type observed for some Y_2O_3-containing Si_3N_4 materials at 1000°C.[7]

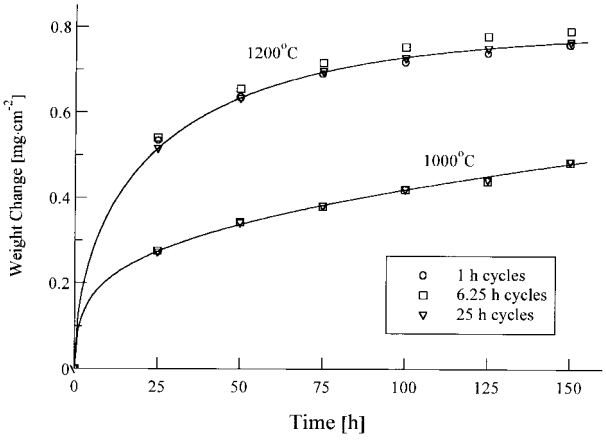

Fig. 1. Effect of thermal cycling on the oxidation kinetics of a 9 wt% Y_2O_3-doped hot-pressed Si_3N_4 at 1000 and 1200°C.

Although at 1000°C, the weight changes for the first 50 h of test were closely similar to those recorded for 50-h isothermal exposures,[10] the isothermal weight gain after 50 h at 1200°C (0.47 mg cm^{-2}) was lower than that for thermally cycled material (0·63–0·65 mg cm^{-2}). The reason for the latter is attributable to differences in scale composition and morphology associated with the pick up of impurities released from the alumina reaction tubes at high temperatures. Indeed, an interesting feature with respect to scale composition was detected. Sodium was detected by EDX in the oxide layers formed on the Si_3N_4 in the thermal cycling apparatus where relatively new alumina furnace internals were used (sodium is found at levels typically up to 100 ppm even in 'high-purity' alumina). Sodium is known to accelerate the oxidation of silicon-based ceramics due to the increased permeation of molecular oxygen through the oxide layers, which is probably associated with the formation of non-bridging oxygens.[11] It is therefore believed that sodium impurities from the alumina furnace furniture are responsible for the enhanced oxidation rates observed.

3.2 Oxidation modelling

In order to evaluate the kinetics of the oxidation process, a number of methods have been used over the years. It is common practice to make an initial assumption based on the fact that because the rate of weight change progressively decreases with time, diffusion is determining the rate control process. If this is true, then a parabolic equation could be fitted to the data. In this case, and in fact many others, the parabolic fit is not a good one.

Kinetics in Fig. 1 are well described by the model developed by Persson *et al.*,[12] over the entire exposure time used, as

$$x = \mathrm{a}\ \arctan\sqrt{bt} + \mathrm{c}\sqrt{t} + \mathrm{d} \qquad (1)$$

although at 1000°C the multiple law model proposed by Nickel[13] can also be applied (Figs 2–4)

$$x = k_{\mathrm{lin}}t + k_p\sqrt{t} + k_{\log}\log t \qquad (2)$$

where the mass change per unit area x is expressed as a function of time t by several constants, i.e. a, b, c and d and the linear (k_{lin}), parabolic (k_p) and logarithmic (k_{log}) rate constants.

The arctan component of eqn (1) is derived by incorporating into the parabolic rate law:

$$x^2 = k_p t + \text{const.} \tag{3}$$

where $x = \Delta m/A$ (i.e. mass change per unit surface area), a function $A(t)$ which describes the decrease of the cross-section area of the amorphous phase available for oxygen diffusion. This model is based on the assumption that the oxygen diffusion through the crystalline phase is negligible compared to that through the amorphous phase. For eqn (2), the linear component would represent surface reactions, the parabolic component would reflect diffusion control and the logarithmic component would describe the effect of progressively decreasing surface area (owing to crystallisation of glassy SiO_2 or bubbles' formation). Diffusion could be of either additive/impurities or oxygen/nitrogen through the surface oxide layer. For this mathematical fit to be possible, the process of oxidation cannot be one of simple diffusion controlled scale growth.

At 1200°C, there was no significant effect of thermal cycling on the weight change data for specimens cycled six, 24 or 150 times and kinetics are best fitted by eqn (1), as illustrated in Fig. 1.

At 1000°C, however, data can be fitted either by eqn (1) or by derivative of eqn (2). Applying eqn (2) to the data and then eliminating components which give a negative value for the rate constant, the method proposed by Nickel,[13] a logarithmic-linear rate law could also be used:

$$W = k_{log} \log t + k_{lin} t \tag{4}$$

with the contribution of the logarithmic component dominating (Fig. 2). The implication is that the formation of crystalline silica leads to a progressive decrease of the effective surface area available for relatively fast diffusion through the amorphous silica, and thus the net weight gain is logarithmic. It should be noted that fitting data at 1000°C with eqn (2) gave a negative k_p value. Since this value does not reflect a physical reality it has been omitted. Nevertheless, attention is drawn to the fact that a logarithmic-parabolic rate law can also fit this set of data, again using the Nickel[13] eqn (2), but not permanently excluding negative constants after the first trial fit:

$$W = k_{log} \log t + k_p \sqrt{t} \tag{5}$$

with the contribution of the logarithmic component dominating (Fig. 3). This highlights the need for caution, and a degree of flexibility, when using the multiple rate law model to fit oxidation data. An incorrect fit will lead to the rate controlling mechanism being wrongly identified and any extrapolation of data beyond the maximum test time would lead to a wrong prediction of the amount of material consumed by the oxidation process. The need to verify whether breaks in kinetics for a particular data set exist also cannot be overemphasised. Indeed, Nickel suggests a method for this also.[13] Unless there is a good reason to believe that a given mechanism is not active, one should not necessarily discharge negative k-values, as demonstrated in this case. Recently, improvements in the application of curve fitting have been published.[14] At this point, the question is to know which is the 'best' fitting? In order to try answering this question, data was gathered for longer exposure time at 1000°C. For this purpose, cycles of 6·25 h were chosen for evaluating the effect of thermal cycling on the kinetics obtained for a total

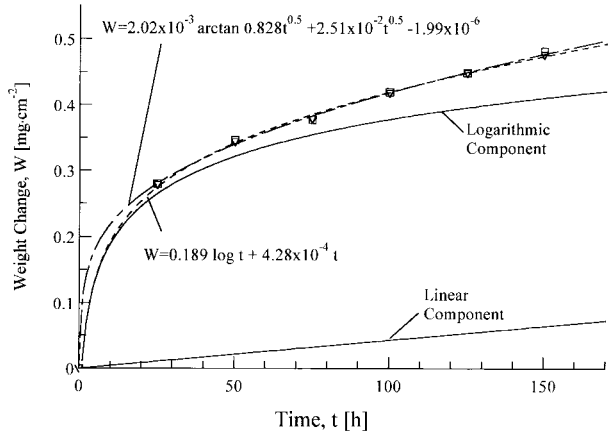

Fig. 2. Fitting of the kinetic data obtained for 150 h of exposure at 1000°C using 6·25 h cycles with both a logarithmic-linear rate law model and the arctan model.

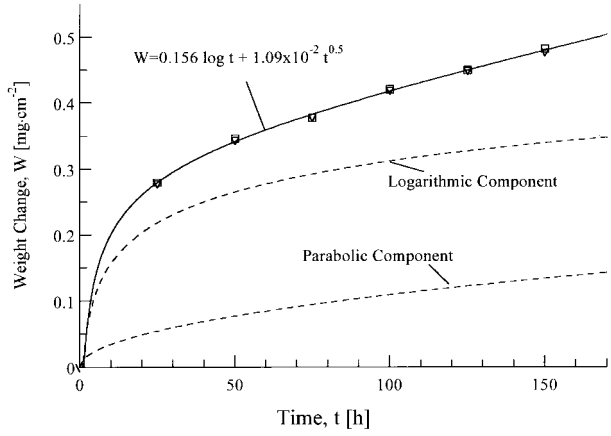

Fig. 3. Fitting of the kinetic data obtained for 150 h of exposure at 1000°C using 6·25 h cycles with a logarithmic-parabolic rate law model.

exposure time of 500 h. The results are shown in Fig. 4. Under these conditions, data obtained can be fitted by eqn (2). This shows that for longer exposure times (500 h), the parabolic contribution becomes progressively more important with increasing time of exposure at 1000°C and suggests that diffusion through the crystalline phases in the surface layer affects the overall process. It follows that short-term rates may not be extrapolated to long times without some knowledge of the evolution of oxidation product morphology. Additionally, this approach to the analysis of oxidation kinetics highlights the need not only to consider multiple fitting models, but that changes of rate controlling mechanism with time will affect the mathematical fit obtained. It is also evident from Fig. 4 that if the logarithmic-linear rate law derived for the first 150 h of exposure [eqn (4) in Fig. 2] would have been considered, an overestimation of the weight changes would have been obtained. The logarithmic-parabolic rate model [eqn (5) in Fig. 3] would have resulted in a slight underestimation of the weight changes actually measured. In addition, it is now possible to use eqn (2)

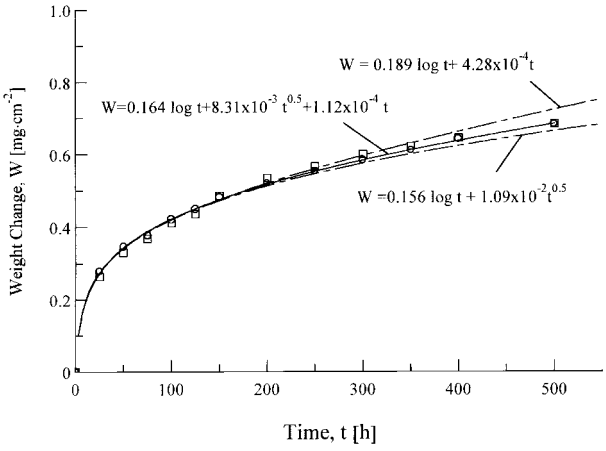

Fig. 4. Fitting of the kinetic data obtained for 500 h of exposure at 1000°C using 6·25 h cycles with a multiple rate law model.

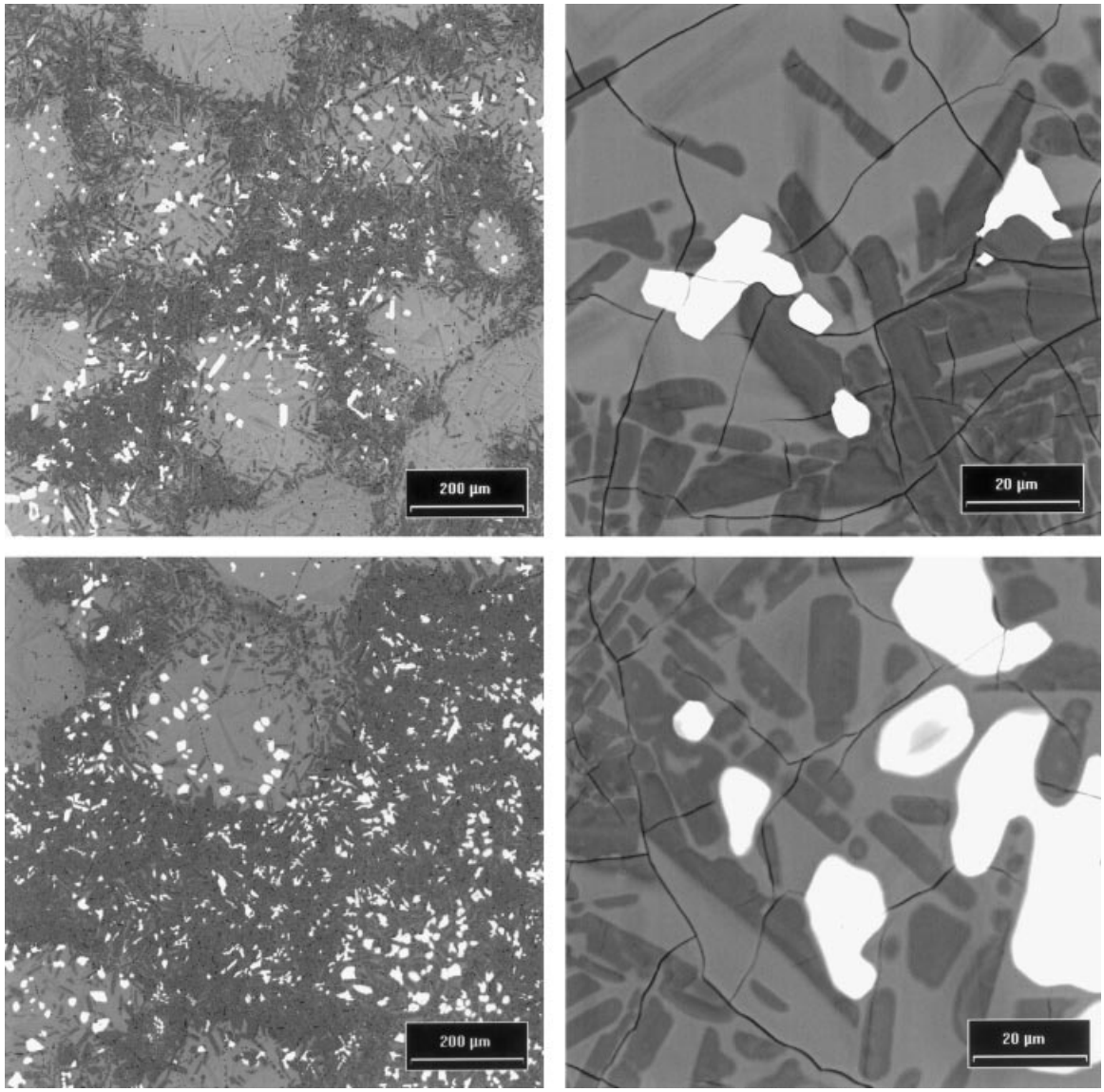

Fig. 5. BSE topographical micrographs of Ceranox NH209 exposed at 1000°C in 'dry' air using 6·25 h cycles for 150 h (top) and 500 h (bottom).

derived from data in Fig. 4 to fit the data obtained for the first 150 h, as well. In summary, this case has demonstrated that in any extrapolation care must be taken when using the multiple law model proposed by Nickel.[13]

3.3 Morphology of oxidation products

The surface of the oxide layer was found to consist of four main features: a glassy phase, dark and bright crystals embedded in the glass and pores (Figs 5–11). Owing to high atomic number contrast possible with back-scattered electrons (BSE), scale morphology, particularly with respect to Y, can readily be observed. The bright areas in the BSE images are attributed to high yttrium content.

The identification of the crystalline oxidation products was established by a combination of XRD and energy dispersive analyses in the SEM.

As the oxidation temperature and time were increased crystals were found to nucleate and grow preferably at the gas/oxide interface (as β-$Y_2Si_2O_7$) and at the nitride/scale interface (mainly SiO_2), the morphology being similar to that described previously for isothermal conditions of oxidation.[15] EDX analyses revealed that the bright crystals contained Y, Si and O and therefore correspond to the needle-like and/or plate-like yttrium silicates ($Y_2Si_2O_7$) identified by XRD. The size and shape of these crystals was found to be dependent on both temperature and cycling frequency. The dark crystals were found by EDX to contain Si and O and thus correspond to SiO_2 crystals (tridymite and cristobalite). In all cases, the glass phase was cracked, which is mainly attributed to the large volume change in the $\beta \rightarrow \alpha$ cristobalite phase transformation on cooling. Finally, some pores, associated with the inability of at least some N_2 to escape by diffusion through the silicate glass, were observed.

Microstructural analyses revealed that there was no apparent difference in morphology of the oxide layer formed at 1000°C using 6·25 and 25 h cycles, respectively. However, it was evident that the volume fraction of crystals (both $Y_2Si_2O_7$ and cristobalite) in the scale increased steadily with time (Fig. 5) and that the crystalline material contributed to the formation of a continuous inner layer within the scale (Fig. 6). Since the rate of diffusion through cristobalite is usually slower than through amorphous silica,[1] the overall rate of oxidation, as measured by weight changes, was less than parabolic, which is in good agreement with the kinetics' fitting described in the previous section.

The existence of cristobalite (the crystalline form of SiO_2 which is stable above 1470°C)[1] at temperatures as low as 1000°C (as indicated by XRD and SEM) suggests that additive and impurity cations (mainly Mg and Ca), found in the glassy surface layer, not only reduce glass viscosity, thereby enhancing devitrification,[16] but also promote ionic mobility. Thus, it is possible that both the additives and impurities present in the bulk ceramic form mixed silicates like (Al, Mg, Ca, Fe)SiO_x in addition to crystalline SiO_2 (both cristobalite and traces of tridymite) as well as yttrium silicates mainly $Y_2Si_2O_7$.

Although there was no significant effect of thermal cycling on the oxidation kinetics at 1200°C, cyclic oxidation influenced the morphology of the oxide layers formed under the chosen conditions. Figure 7 illustrates this finding. It appears that any cracks induced by thermal cycling heal immediately on re-exposure to high temperatures, as in the case of 1000°C, possibly owing to the vitreous nature of the oxide layers formed. These glasses were found by EDX to contain sodium, probably as a result of reaction tube contamination effects. Such an effect

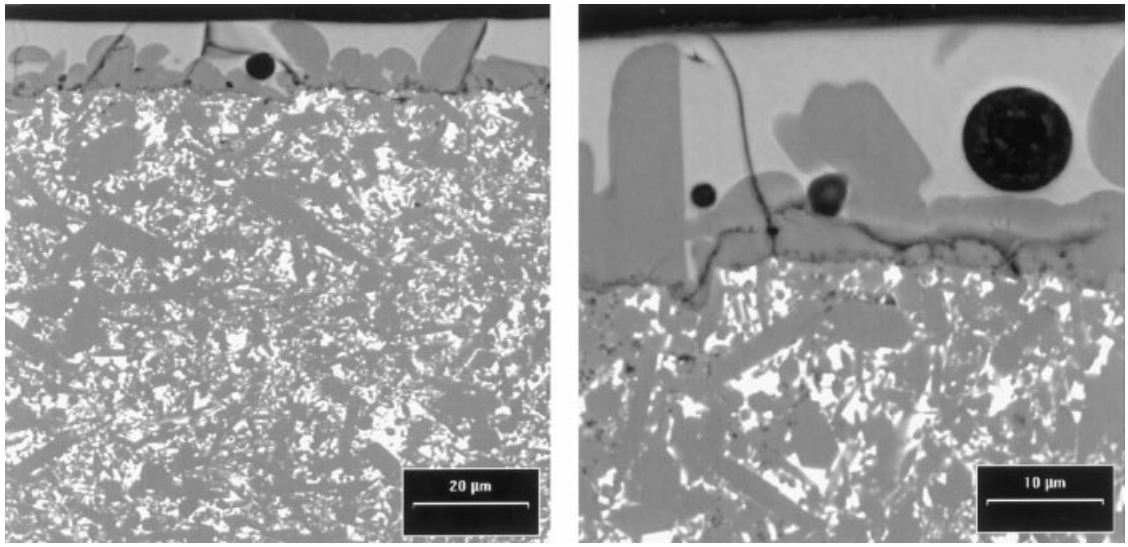

Fig. 6. BSE cross-sections of Ceranox NH209 exposed for 150 h at 1000°C in 'dry' air using 6·25 h cycles for 150 h (left) and 500 h (right). (Note that in all micrographs the surface oxide film is shown at the top part of the images.)

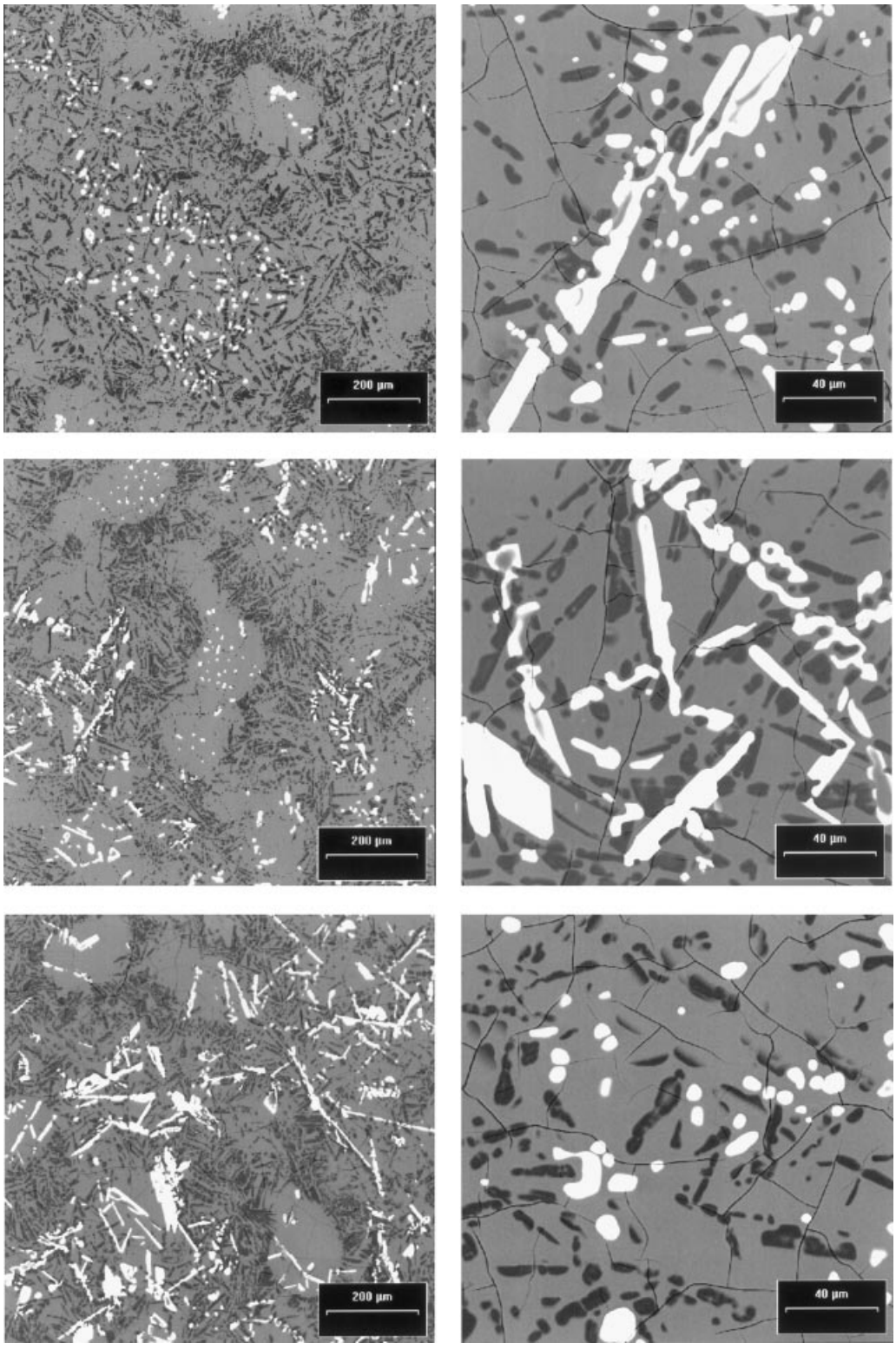

Fig. 7. BSE topographical micrographs of Ceranox NH209 exposed at 1200°C in 'dry' air for 150 h using 1 h cycles (top), 6·25 h cycles (middle) and 25 h cycles (bottom).

has already been noted by Opila[17] who suggested that high temperature oxidation studies of silica formers should be conducted in quartz tubes rather than in alumina tubes. An ageing effect for impurities (particularly sodium) in the alumina has been observed and only for long exposure times (> 2000 h) at temperatures above 1200°C, impurity effects on oxidation kinetics became insignificant relative to oxidation in fused quartz tubes.

Cracks induced by cyclic oxidation on the oxide layers were usually found to initiate at the nitride/oxide layer interface. These cracks were found to grow outwards through the oxide layer. No evidence of crack propagation in the bulk ceramic was ever observed. At places, crack growth resulted in fracture of yttrium silicates as illustrated in Fig. 8.

The concentration of yttrium silicate crystals has been found to decrease with increasing cycle

frequency. This is probably related to the effect of heating and cooling on the dissolution/precipitation processes of these crystals in the silicate glass formed at this temperature. At shorter exposure times (50 h), the morphology of the oxide layer differs from that obtained for longer exposure times (150 h) as shown in Fig. 9. It can be seen that SiO_2 crystals tend to develop a plate-like morphology whereas yttrium silicate crystals showed both globular, needle-like and dendrite-type morphologies. Both the thin needle-like and dendrite-like crystals possibly precipitate from the silicate glass on cooling. It has also been noted that the Y-containing crystals were randomly distributed after thermal cycling in contrast to the preferential nucleation in the outer part of the layer, which is usually observed after isothermal exposure. Figure 10 shows that gas bubbles within the silicate glass act as nucleation sites for yttrium silicate precipitates on cooling.

Figure 11 shows that the surface of the test pieces cycled for 25 h at 1200°C consists of a double layer, the outer part being mostly amorphous and the inner part mostly crystalline SiO_2. Yttrium silicates were found embedded in the outer part of the glass. In some places, partial dissolution of some of the needle-like crystals in the surrounding glass took place as illustrated in Fig. 7 (bottom). With increasing number of cycles, the morphology of the yttrium silicate crystals changed progressively from plate-like and needle-like to globular. The mechanism responsible for this change in morphology is

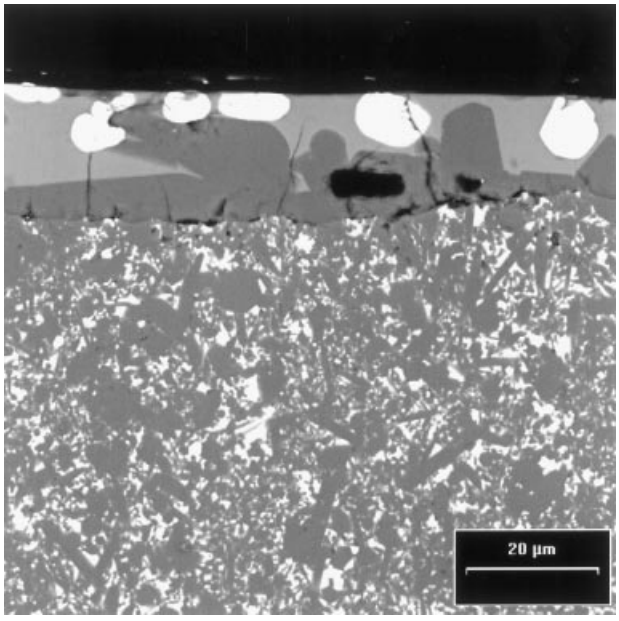

Fig. 8. BSE cross-sections of Ceranox NH209 exposed for 150 h at 1200°C in 'dry' air using 6·25 h cycles. (Note that in this micrograph the surface oxide film is shown at the top part of the image.)

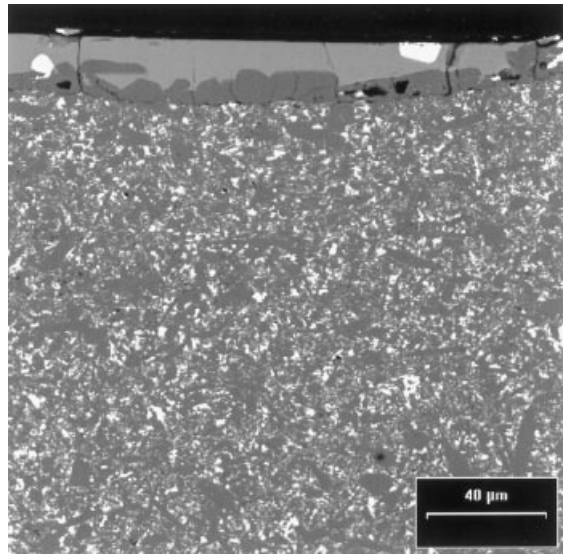

Fig. 10. BSE cross-section of Ceranox NH209 exposed for 50 h at 1200°C in 'dry' air using 1 h cycles. (Note that in this micrograph the surface oxide film is shown at the top part of the image.)

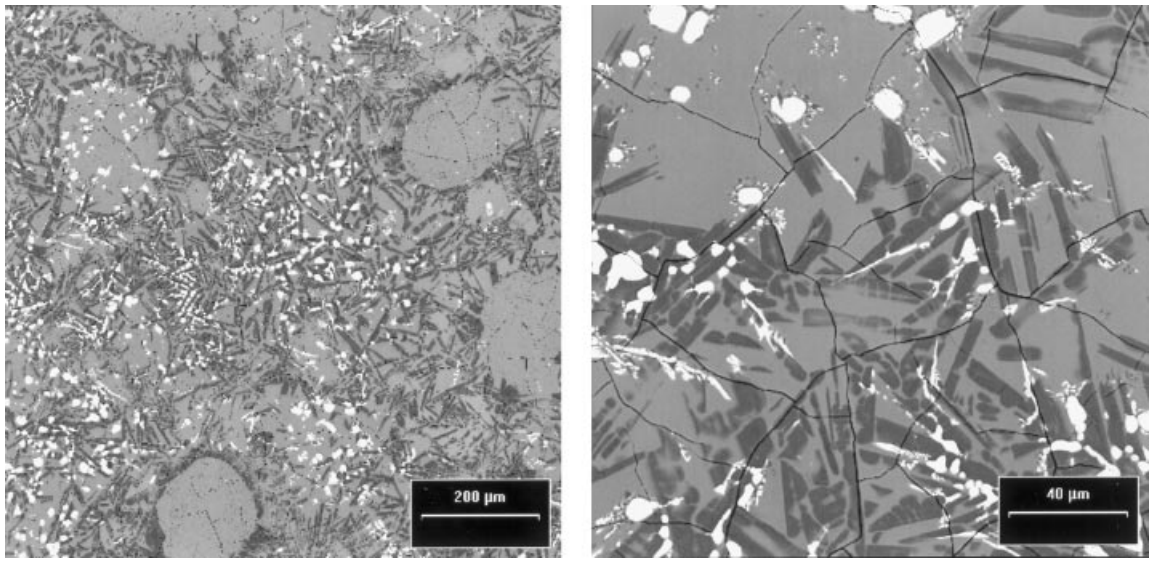

Fig. 9. BSE topographical micrographs of Ceranox NH209 exposed for 50 h at 1200°C in 'dry' air using 1 h cycles.

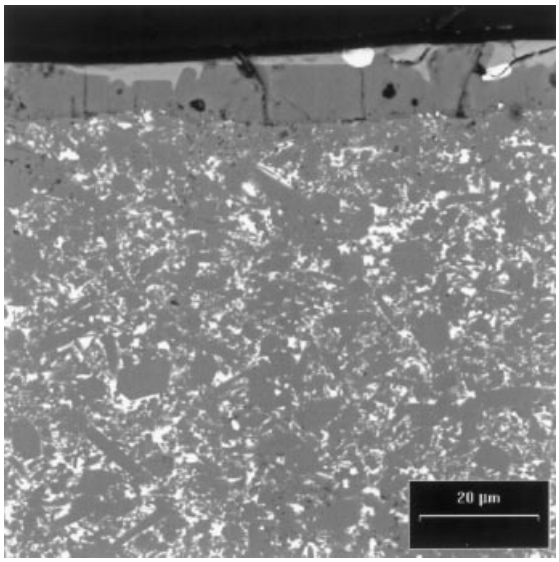

Fig. 11. BSE cross-section of Ceranox NH209 exposed for 150 h at 1200°C in 'dry' air using 25 h cycles. (Note that in this micrograph the surface oxide film is shown at the top part of the image.)

not known, but thermal cycling probably increases the abundance of nucleation sites for yttrium silicate crystals in the silicate glass. The frequency of cycling also influences the crystallisation rate and morphology of the SiO_2 crystals. It was noted that the size of the SiO_2 crystals decreases with increasing of the number of cycles. Also the morphology of the SiO_2 crystals gradually changed from acicular (Fig. 7, bottom) to globular (Fig. 7, top).

Deviations from non-parabolic behaviour can be attributed to crystallisation of the oxidation layer since the effective surface area, through which the oxidant can attack is reduced over time. Although a lot of scatter is reported in the literature for diffusion data, it is clear that the diffusion rate of oxygen in crystalline SiO_2 is slower than in amorphous SiO_2.[1] Crystallisation of some of the amorphous SiO_2 first formed on Si_3N_4 not only causes a progressive decrease of the cross-section area available for faster molecular oxygen diffusion through the glass but also reduces the solubility and permeability of both oxygen and nitrogen. The effective O_2 diffusion coefficient in the oxide film decreases with an increasing amount of devitrified phases with time. Moreover, the presence of impurities in the intergranular phase causes an increase in the rate of crystallisation of silicon dioxide glasses and thus a decrease of the oxidation rate with time. Additionally, a reduction in nitrogen mobility in crystalline SiO_2 can lead to the formation of bubbles at the nitride/oxide interface as outward transport of N_2 is inhibited. If the N_2 pressure builds up, cracking of a continuous crystalline SiO_2 layer may occur providing direct access of oxygen to unoxidised ceramic. Thus a change from a diffusion-controlled process to an interfacial reaction controlled process would be anticipated for at least a fraction of the surface area of the test piece. Lange *et al.*[6] showed that the quaternary compounds formed within the Si_3N_4–Y_2O_3–SiO_2 system readily oxidise when exposed to oxidising environments at high temperatures. Moreover, oxidation kinetics obtained for one of these phases (i.e. $Si_3Y_2O_3N_4$) were found to be linear due to cracking of the material caused by large volume changes on oxidation. Thus, the overall oxidation rate may be influenced by a combination of diffusion processes and interface reactions; with the contribution from diffusion being dominant. This reasoning may explain the linear contribution for the overall oxidation kinetics model used to fit data in Figs 2 and 4. Therefore, polyphase Si_3N_4 ceramics are very unlikely to follow simple oxidation rate laws because of the change in properties of the oxide layer with time. This approach to the analysis of oxidation kinetics highlights the need not only to consider multiple fitting models, but that changes of rate controlling mechanism with time will affect the mathematical fitting obtained. An incorrect fit will lead to the rate controlling mechanism being wrongly identified. Care must be taken because more than one single oxidation mechanism is most probably acting during oxidation making it difficult to predict long term behaviour. The fact that the oxidation process changes with time of exposure would render any data extrapolated beyond the maximum time actually tested potentially unreliable. Moreover, regardless of the frequency of thermal cycling, oxidation kinetics based on weight change, are constant at a given exposure temperature.

4 Conclusions

From a study of the oxidation in 'dry' air of a Y_2O_3-containing hot-pressed silicon nitride under both isothermal and thermal cycling conditions, the following conclusions can be drawn:

1. It has been shown that the oxidation resistance depends on the formation of a protective SiO_2-rich layer but temperature and thermal cycling frequency influence the exact composition and morphology of the layer.
2. Cyclic oxidation seems to have little effect on the oxidation kinetics, based on weight change data. While thermal cycling caused cracking of the surface layers, neither loss of oxidation product material (spallation) nor accelerated rates of oxidation were observed. This suggests that cracks induced on cooling heal immediately upon re-exposure to high temperature,

independent of both the frequency of thermal cycling and the exposure temperature. However, cyclic oxidation affects the morphology of the crystalline phases formed within the oxide layer.

3. The exposure of the material at 1000°C did not result in catastrophic oxidation, as observed for other Y_2O_3-doped hot pressed Si_3N_4 compositions, even under thermal cycling conditions.
4. Crystallisation of some of the amorphous SiO_2 first formed on Si_3N_4 with time (enhanced by the presence of the intergranular phase) leads to deviations from the parabolic rate law owing to reduced rates of diffusion through the crystalline material.
5. This study has shown that the oxidation mechanism is time dependent. As a consequence care must be taken in any mathematical modelling of oxidation kinetics. Only a close correlation of kinetic data and composition and morphological information can enable adequate characterisation of oxidation behaviour to be achieved.

Acknowledgements

One of the authors (F.C.O.) wishes to thank the European Commission for a post-doctoral grant. The assistance provided by J. Ungeheuer, J. Van Eijk, P. Frampton and K. Schuster is acknowledged. This work was carried out within the European Commission's Research and Development Programme.

References

1. Lamkin, M. A., Riley, F. L. and Fordham, R. J., Oxygen mobility in silicon dioxide and silicate glasses: a review. *J. Eur. Ceram. Soc.*, 1992, **10**, 347–367.
2. Weaver, G. Q. and Lucek, J. W., Optimization of hot-pressed Si_3N_4–Y_2O_3 materials. *Am. Ceram. Soc. Bull.* **57** (1978) 1131–1134, 1136.
3. Maeda, M., Nakamura, K., Ohkubo, T., Ito, M. and Ishii, E., Oxidation behaviour of silicon nitride under cyclic and static conditions. *Ceramics International*, 1989, **15**, 247–253.
4. Echeberría, J. and Castro, F., Comparison between continuous and cyclic oxidation of fully dense Si_3N_4 + 1 wt% Y_2O_3. In *Proceedings of the 11 Risø International Symposium on Metallurgy and Material Science: Structural Ceramics—Processing, Microstructure and Properties*, ed. J. J. Bentzen, J. B. Bilde-Sørensen, N. Christiansen, A. Horsewell and B. Ralph. Risø National Laboratory, Denmark, 1990, pp. 249–255.
5. Gazza, G. E., Hot-pressed Si_3N_4. *J. Am. Ceram. Soc.*, 1973, **56**, 662.
6. Lange, F. F., Singhal, S. G. and Kuznicki, R. C., Phase relations and stability studies in the Si_3N_4–SiO_2–Y_2O_3 pseudoternary system. *J. Am. Ceram. Soc.*, 1977, **60**, 249–252.
7. Patel, J. K. and Thompson, D. P., The low-temperature oxidation problem in yttria-densified silicon nitride ceramics. *Br. Ceram. Trans. J.*, 1988, **87**, 70–73.
8. Lange, F. F., Silicon nitride polyphase systems: fabrication, microstructure, and properties. *International Metals Reviews*, 1980, **25**, 1–20.
9. Costa Oliveira, F. A., Tambuyser, P. and Baxter, D. J., Microstructure of a yttria-doped hot-pressed silicon nitride, *Ceram. Int.*, accepted.
10. Costa Oliveira, F. A., Baxter, D. J. and Ungeheuer, J., The oxidation kinetics of a yttria-doped hot-pressed silicon nitride. In *Key Engineering Materials*, Vols 132–136. Trans Tech Publications, Aedermansdorf, Switzerland, 1997, pp. 1580–1583.
11. Zheng, Z., Tressler, R. E. and Spear, K. E., The effect of sodium contamination on the oxidation of single crystal silicon carbide. *Corros. Sci.*, 1992, **33**, 545–556.
12. Persson, J., Käll, P. and Nygren, M., Interpretation of the Parabolic and Nonparabolic oxidation behavior of silicon oxynitride. *J. Am. Ceram. Soc.*, 1992, **75**, 3377–3384.
13. Nickel, K. G., Multiple law modelling for the oxidation of advanced ceramics and a model-independent figure of merit. In *Corrosion of Advanced Ceramics: Measurement and Modelling*, vol. 267, ed. K. G. Nickel. NATO ASI Series E. Kluwer Academic, Dordrecht, The Netherlands, 1994, pp. 59–71.
14. Ogbuji, L. U. J. T., Subparabolic oxidation behaviour of silicon carbide at 1300°C. *J. Electrochem. Soc.*, 1989, **145**, 2876–2882.
15. Nickel, K. G., Oxidation and corrosion of advanced ceramics. *Powder Metallurgy International*, 1989, **21**, 29–34.
16. Singhal, S. C., Thermodynamics and kinetics of oxidation of hot-pressed silicon nitride. *J. Mat. Sci.*, 1976, **11**, 500–509.
17. Opila, E., Influence of alumina reaction tube impurities on the oxidation of chemically-vapor-deposited silicon carbide. *J. Am. Ceram. Soc.*, 1995, **78**, 1107–1110.